*Proc. Natl. Acad. Sci. USA*
Vol. 76, No. 8, pp. 3585–3589, August 1979
Chemistry

# Dynamics of activated processes in globular proteins

(side-chain rotation in proteins/transition state theory/catalysis/Monte Carlo and molecular dynamics method)

J. A. McCammon* and M. Karplus

Department of Chemistry, Harvard University, Cambridge, Massachusetts 02138

*Contributed by Martin Karplus, May 16, 1979*

**ABSTRACT** **A procedure for the dynamical simulation of activated processes, such as ligand binding and enzymatic reactions, in a globular protein is outlined. Preliminary calculations of the transition state geometry and barrier crossing trajectories are presented for a model reaction, the rotation of an aromatic ring in the bovine pancreatic trypsin inhibitor. The results show that repulsive nonbonded interactions between the ring atoms and the atoms in the surrounding protein matrix determine the dynamical character of the reorientation process; the nonbonded interactions are the source of the rotational barrier and of the impulses that speed up or slow down the ring motion during the barrier crossings.**

Activated processes play an important role in enzymatic reactions and more generally in the dynamics of protein molecules (1). In an activated process, the observed rate is limited by an energy barrier between the initial and the final state. Most processes in native proteins that take place on a time scale of microseconds or longer are likely to involve such an activation step. Measurements have yielded information concerning the free energy barriers associated with a variety of activated processes in proteins; these include the rotations of aromatic side chains (2–4), the motion of diatomic ligands through the globin of heme proteins (5, 6), and the interconversion of substrate and product in enzymes such as triosephosphate isomerase (7). For the cases listed the number and magnitudes of the free energy barriers involved have been determined (4–7). Further, measurements of the temperature dependence of the rates have demonstrated that there are large entropies of activation that point to the participation of the protein degrees of freedom in the activated process (3–6).

The availability of these and other data suggests that an investigation of the detailed dynamics of activated processes in proteins is in order. Of primary interest are the protein contributions to the barriers and the dynamics of the motion across the barriers in the interior of a protein. In some cases (e.g., enzymatic reactions) the protein–substrate interactions may act to lower the activation barrier, whereas in others (e.g., ligand penetration) the interactions are themselves the source of the barrier. Because of the mobility of the interior of a protein (8), the measured barriers correspond to an average over a range of instantaneous interactions. Transient relaxation effects due to concerted displacements of the protein atoms may significantly lower the effective barriers. Because the density of proteins is high (9), frictional damping can occur during the transition and lead to diffusional rather than inertial barrier crossings (10–12).

To provide a microscopic description of activated processes in proteins, it will be necessary to carry out a detailed analysis of the dynamics of the atoms involved. In one approach to the problem, which is essentially static in character, empirical energy functions have been used to estimate the activation barriers for 180° rotation ("flips") of the rings of the eight aromatic side chains of the bovine pancreatic trypsin inhibitor (PTI) (13, 14). Such studies have demonstrated the essential role of protein structural relaxation in the rotation of the rings. Only by minimizing the protein energy for each ring orientation were the calculated rotation barriers in good agreement with the NMR measurements (3, 4); the barriers obtained for a rigid protein matrix were much too large. From these static treatments it is clear that to determine the rate of an activated process inside a protein it is necessary to include the correlated atomic displacements that can occur.

The alternative approach to motion in proteins is dynamic in character. The trajectories for the component atoms are determined by solving the simultaneous classical equations of motion with forces evaluated from empirical energy functions and with average kinetic energies corresponding to a given temperature. The atomic motions that take place in the integration period of 10–100 ps have been analyzed in a study of PTI (8, 15). The simulation revealed a wide variety of motional phenomena that occur at ordinary temperatures. In particular, the orientation fluctuations of two tyrosine rings in the neighborhood of their local minima were analyzed in some detail (16). It was shown that the torsional motion is significantly damped by nonbonded interactions of the rings with the surrounding atoms of the protein matrix. This suggests that frictional effects can be large enough to influence the nature of activated structural transitions and that they might be detected in the 180° rotations of aromatic rings.

A dynamics simulation of the type described above does not allow one to study activated processes directly because they are by their nature rare events. It is impossible to obtain many barrier crossing trajectories for an activated process with a rate constant less than $\approx 10^{11}$ $s^{-1}$ in a simulation of length 10–100 ps. Although static reaction-path studies do provide an approximate value for the energy barrier, they cannot give information concerning the dynamics of the activated process. To overcome the limitations of standard reaction path and molecular dynamics calculations, a synthesis of these techniques with the widely used concepts of transition state theory can be employed. Such an approach has been applied to small-molecule collision dynamics (17, 18) and more recently to vacancy diffusion dynamics in regular solids (19). The first step in such a calculation is the determination of a transition region in which a dividing surface between reactants and products can be defined. It is then necessary to generate a set of configurations in this region with coordinate values (other than the ones specifying the region) in accord with a Boltzmann distribution for the temperature under consideration. Given the transition-state configurations, two quantities have to be evaluated. The first is the probability that a system composed of reactants at equilibrium will be in the transition region (in transition state theory,

The publication costs of this article were defrayed in part by page charge payment. This article must therefore be hereby marked "*advertisement*" in accordance with 18 U. S. C. §1734 solely to indicate this fact.

Abbreviation: PTI, bovine pancreatic trypsin inhibitor.

* Present address: Department of Chemistry, University of Houston, Houston, TX 77004.

this corresponds to the equilibrium constant between the activated complex and the reactants), and the second is the probability that the transition-state configurations with appropriate atom velocities will go on to give product (in transition state theory, this corresponds to the transmission coefficient, $\kappa$). Although various aspects of this procedure (sometimes referred to as "phase-space/trajectory calculations") can be done analytically in simple cases, the complexity and multidimensionality of a protein reaction requires that the problem be solved numerically by appropriate combinations of Monte Carlo and molecular dynamics techniques.

In this paper, a preliminary attempt is made to apply the phase-space/trajectory technique to the model problem of the 180° rotation of a tyrosine ring in PTI. The system studied consisted of the 454 heavy (nonhydrogen) atoms of PTI and four internal water molecules; hydrogen atoms were included implicitly by a suitable adjustment of heavy atom parameters. The calculations were based on an empirical energy function composed of a sum of terms associated with bond lengths, bond angles, dihedral angles, hydrogen bonds, and nonbonded (van der Waals and electrostatic) interactions (13, 16, 20). We focus here on the determination of the transition region, the generation of configurations in that region, and the ring reorientation dynamics of these configurations. For specific study we chose Tyr-35, whose aromatic ring is buried in the interior of PTI. Because the rotational barrier is known to be dominated by nonbonded interactions between ring atoms and those of the surrounding protein (13, 16), this case is an ideal example for examining the dynamics of a process in which the effects of protein relaxation and frictional damping are important.

## TRANSITION STATE SAMPLING

Sets of transition state configurations were generated by a combination of molecular dynamics (21) and Monte Carlo procedures (22). Because the arrangement of atoms around the tyrosine is expected to vary significantly due to the normal fluctuations that occur at equilibrium in the native protein, two sets of coordinates were chosen from a molecular dynamics simulation (16) at $T$ = 308 K. The first of these was from the beginning of the run (after 4.9 ps of equilibration) and the second from the end of the run (9.8 ps later). The average root mean square atomic position fluctuation was 0.9 Å, which provides an indication of the variation of the tyrosine environment in the protein at room temperature. To obtain a configuration in the transition region from the first coordinate set, the Tyr-35 ring was rigidly rotated until the dihedral angle $\chi^2_{35}$ = 180°; this would be near the barrier maximum due to the local dipeptide potential (20) ($\chi^2_{35}$ = 71° in the starting coordinates). Close nonbonded contacts in the resulting structure were relaxed by a modified Metropolis Monte Carlo method (22) in which trial conformations were generated by randomly displacing successive atoms within a cube of side 0.09 Å. Atoms which were within 10 Å of $C^{\gamma}_{35}$ in the initial coordinates were sampled more frequently than the remaining atoms (70% of the trial displacements involved one of these atoms, compared to 40% if all atoms were sampled with equal probability); this procedure speeds up relaxation, but still yields a Boltzmann distribution of configurations. To hold the ring in its unstable orientation in the transition region, trial conformations in which $|\chi^2_{35} - 180°| > 2.5°$ were rejected. With $T$ = 300 K, approximately half of the trial conformations were accepted. The potential energy of the protein fell rapidly from an initial value of about 750 kcal/mol (1 kcal = 4.18 kJ) during the first 10,000 steps and decreased more gradually during the subsequent 200,000 steps (see Fig. 1*a*). At this point, trial trajectory calculations were performed (see *Trajectory Calculations*) for two

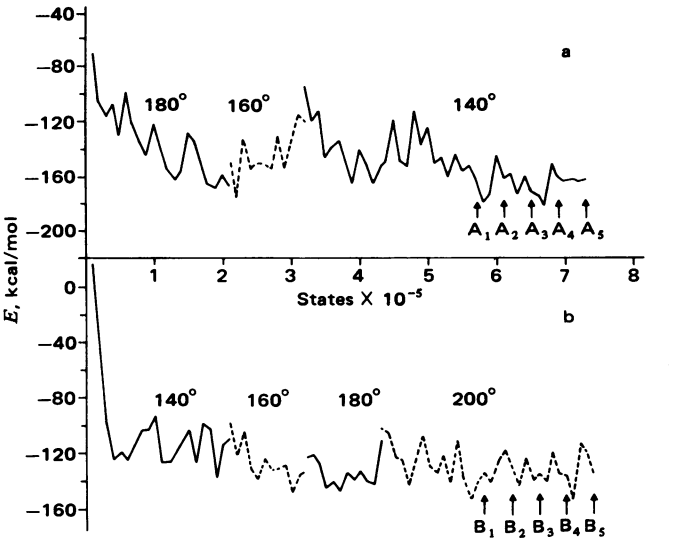


FIG. 1. Potential energy of successive configurations of PTI generated by the Monte Carlo calculations. Points are plotted at intervals of 10,000 steps. Angles above segments of plots indicate values near which $\chi^2_{35}$ was constrained. Arrows indicate configurations used in trajectory calculations. (*a*) The "A" series. (*b*) The "B" series.

relaxed conformations with $\chi^2_{35} \approx 180°$. These trajectories, which failed to exhibit barrier crossings by the ring, suggested that the actual barrier in the ring rotational potential due to the protein contacts was located at $\chi^2_{35} < 180°$. The Monte Carlo calculations were therefore continued by rigidly rotating the ring to $\chi^2_{35}$ = 160° and carrying out further computations as described above with a rejection criterion $|\chi^2_{35} - 160°| > 2.5°$. Because trial trajectories again failed to exhibit barrier crossings by the ring, the Monte Carlo calculations were continued with $\chi^2_{35} \approx 140°$. In this region, successful trial trajectories were obtained, so that this region was chosen as a transition state. Constrained Monte Carlo calculations were continued in the region to generate configurations for detailed trajectory study (set "A"). The potential energy variations during the sequence of Monte Carlo calculations is shown in Fig. 1*a*.

The second set of transition state configurations (set "B") was generated by a corresponding procedure from the later dynamic coordinates. The transition region angle was found to be $\chi^2_{35} \approx 200°$; this second Monte Carlo series is summarized in Fig. 1*b*.

## TRAJECTORY CALCULATIONS

To compute a trajectory that passes through a given transition state configuration, it is necessary to assign initial velocities to all of the atoms. With these positions and velocities as initial conditions, one half of the trajectory (e.g., the ring falling from the transition state into the final state valley) was determined by a molecular dynamics calculation including motion of all of the protein atoms (16). The other half of the trajectory (e.g., the ring rising from the initial state valley to the transition state) was obtained by using the velocities with opposite signs as the initial conditions, calculating the corresponding trajectory by the molecular dynamics method and reversing it in time.

For the study reported here, the velocity assignments were carried out in the following manner. A local reaction coordinate for ring rotation was defined (16) as the torsional angle of the best plane through the ring atoms about the axis which passes through $C^{\gamma}_{35}$ and $C^{\zeta}_{35}$. Reaction coordinate velocities (i.e., torsional angular velocities for the ring) were specified by assigning velocities perpendicular to the plane of the ring for the atoms $C^{\delta 1}_{35}$, $C^{\delta 2}_{35}$, $C^{\epsilon 1}_{35}$, $C^{\epsilon 2}_{35}$; these velocities had equal magnitudes, and

the signs were consistent with overall ring rotation. The magnitudes of these velocities were chosen by sampling an effusion velocity distribution (23) for the torsional motion to obtain the proper weighting for determining a transition rate (18). Velocities for all other atoms of the protein, and for the in-plane motions of the above four atoms, were chosen by sampling a Maxwellian distribution (18, 23). Both distributions corresponded to 300 K. This procedure, which involves separation of the ring initial torsional velocities from the rest of the protein, is a simplification corresponding to the assumption that the protein has infinite mass and moment of inertia, and that the aromatic ring is effectively rigid (24).

With the procedure outlined above, five trajectories were calculated for each of the two transition state sets; the configurational starting point is indicated as $A_1$–$A_5$, $B_1$–$B_5$ in Fig. 1. Integration of the simultaneous equations of motion for the entire protein was performed by means of the Gear algorithm (16, 25) with time steps of $9.78 \times 10^{-16}$ s. The kinetic energy in the transition configuration associated with the angular motion varied from 0.16 to 1.44 kcal/mol. The total length of each trajectory was 1.17 ps; it required 10 min of IBM 360/91 computer time.

## RESULTS

In this section, we present some of the significant aspects of the two transition regions and of the trajectories calculated in the two regions.

### Transition regions

The transition configurations generated within each series (set A or set B) show qualitative similarities, but there are important differences between the two series. In the A series, the local density of atoms around the Tyr-35 ring is somewhat higher than in the B series. The average number of heavy atoms within 5 Å of a Tyr-35 ring carbon is close to 20 (excluding atoms directly bonded to the ring) for series A; the corresponding numbers for the B series and for the x-ray structure (26) are 17 and 21, respectively.

The substantial difference in $\chi^2_{35}$ for the two sets of transition states results from the dominant role played by local backbone atoms and other nearby atoms of the protein in determining the shape of the potential energy barrier to ring rotation. The neighboring protein matrix atoms whose repulsive nonbonded contacts with the ring atoms are important in determining the $\chi^2_{35}$ values of the two transition regions are shown in Table 1. The atoms listed are those that exert the most significant torques about the $C^{\gamma}_{35}$–$C^{\zeta}_{35}$ ring axis in the Monte Carlo series from which the transition configurations were selected. The values of the torques are obtained by averaging over the final 200,000 steps of each Monte Carlo series. It can be seen that most of the interactions are with local backbone atoms ($C^{\alpha}_{35}$, $C_{35}$, $N_{36}$, $C_{36}$, $O_{36}$), but that spatial neighbors ($O_{10}$, $O_{37}$, $O_{39}$) and one of the internal water molecules contribute as well.

Table 1. Nonbonded interactions in transition states

| A series | | B series | |
|---|---|---|---|
| Atom pair | Torque, kJ/mol | Atom pair | Torque, kJ/mol |
| $C^{\delta 1}_{35}$–$O_{10}$ | 14.9 | $C^{\delta 2}_{35}$–$N_{36}$ | −9.2 |
| $C^{\delta 2}_{35}$–$N_{36}$ | −13.3 | $C^{\epsilon 1}_{35}$–$O_{39}$ | 6.7 |
| $C^{\delta 1}_{35}$–$W_5$ | 5.7 | $C^{\delta 2}_{35}$–$C_{36}$ | −5.4 |
| $C^{\delta 2}_{35}$–$C^{\alpha}_{35}$ | −4.1 | $C^{\delta 1}_{35}$–$W_5$ | −3.9 |
| $C^{\epsilon 2}_{35}$–$O_{37}$ | 3.5 | $C^{\delta 2}_{35}$–$C_{35}$ | −3.0 |
| $C^{\epsilon 1}_{35}$–$W_5$ | 2.6 | $C^{\delta 2}_{35}$–$C^{\alpha}_{35}$ | 2.5 |
| $C^{\delta 2}_{35}$–$C_{36}$ | 1.4 | $C^{\delta 2}_{35}$–$O_{36}$ | −1.7 |

$W_5$ is a solvent water molecule.

Monte Carlo averages were calculated also for bond angles and dihedral angles of Tyr-35 to determine the strains in these internal coordinates in the two sets of transition states. The results are compared in Table 2 with those obtained in the energy-refined geometry (13). Except for $C_{35}$–$C^{\alpha}_{35}$–$C^{\beta}_{35}$ in the A series, the bond angle deformations correspond to increases in the bond angles of the sequence of atoms comprising $C^{\delta 2}_{35}$, $C^{\gamma}_{35}$, $C^{\beta}_{35}$, $C^{\alpha}_{35}$, $C_{35}$, $N_{36}$. These deformations serve to relieve the stress arising from the nonbonded repulsion between $C^{\delta 2}_{35}$ and $N_{36}$. The associated bond angle stresses in the Monte Carlo averages amount to 5–10 kcal/mol, which is similar to the stresses found in the static barrier calculations (13). The dihedral angle deformations ($\phi_{35}$, $\psi_{35}$, $\chi^1_{35}$) seem to involve a more complicated set of interactions, arising from both near-neighbor (e.g., $C^{\delta 2}_{35}$–$N_{36}$) and longer range repulsion.

### Trajectories

All of the 10 sample molecular dynamics trajectories resulted in successful crossing of the potential energy barrier for ring rotation. The times required for a complete ring reorientation range from 0.5 to 1.0 ps. In every case the ring torsional angle increased monotonically with time during the barrier crossing. However, there are some significant differences in the detailed time variations of the angle. In seven trajectories, the angular motion corresponded to that expected for a simple barrier; that is, the ring slowed down somewhat when the ring was near the top and then sped up as the ring moved down the far side. Fig. 2*a* shows the time variations of the ring torsional angle and torsional angular velocity for one such case, trajectory $B_5$. In the other three trajectories (two in series A and one in series B), the torsional motion of the ring was nearly stopped one or more times during the barrier crossings; an example is trajectory $A_5$ (Fig. 3*a*).

A detailed analysis shows that the torsional motion of the ring in every trajectory can be accounted for in terms of nonbonded repulsions between ring and protein matrix atoms. More specifically, the total impulse due to the resulting torques that exceed $10^{11}$ erg/mol in magnitude at any instant is nearly equal to the observed angular momentum change of the ring during the interval over which these torques act. The time variations of all such torques acting during trajectories $B_5$ and $A_5$ are shown in Figs. 2*b* and 3*b*, respectively. Analyses of these figures and corresponding ones for the other trajectories show that most of these torques have substantial magnitudes only for rather short intervals ($\lesssim$0.1 ps). Significant roles in promoting and opposing the ring rotations are played by backbone atoms of residues 35 and 36 as well as atoms that are more distant in the primary structure (Table 3). Particular matrix atoms tend to have similar effects within the trajectories of each set, but some different atoms are involved in the two sets. Certain matrix atoms switch from rotation-opposing to rotation-promoting roles as the ring squeezes by them in a given trajectory (e.g., $N_{36}$ in both sets).

Table 2. Structural features of transition states

| Internal coordinate | Angle, ° | | |
|---|---|---|---|
| | ERG* | A series | B series |
| $C^{\beta}_{35}$–$C^{\gamma}_{35}$–$C^{\delta 1}_{35}$ | 120.7 | 117.6 | 116.7 |
| $C^{\alpha}_{35}$–$C^{\beta}_{35}$–$C^{\gamma}_{35}$ | 114.5 | 117.9 | 120.5 |
| $C_{35}$–$C^{\alpha}_{35}$–$C^{\beta}_{35}$ | 114.1 | 109.1 | 118.9 |
| $N_{36}$–$C_{35}$–$C^{\alpha}_{35}$ | 111.1 | 113.9 | 116.5 |
| $\phi_{35}$ | 271 | 258 | 296 |
| $\psi_{35}$ | 133 | 139 | 115 |
| $\chi^1_{35}$ | 172 | 186 | 164 |

* Energy-refined geometry (see ref. 13).

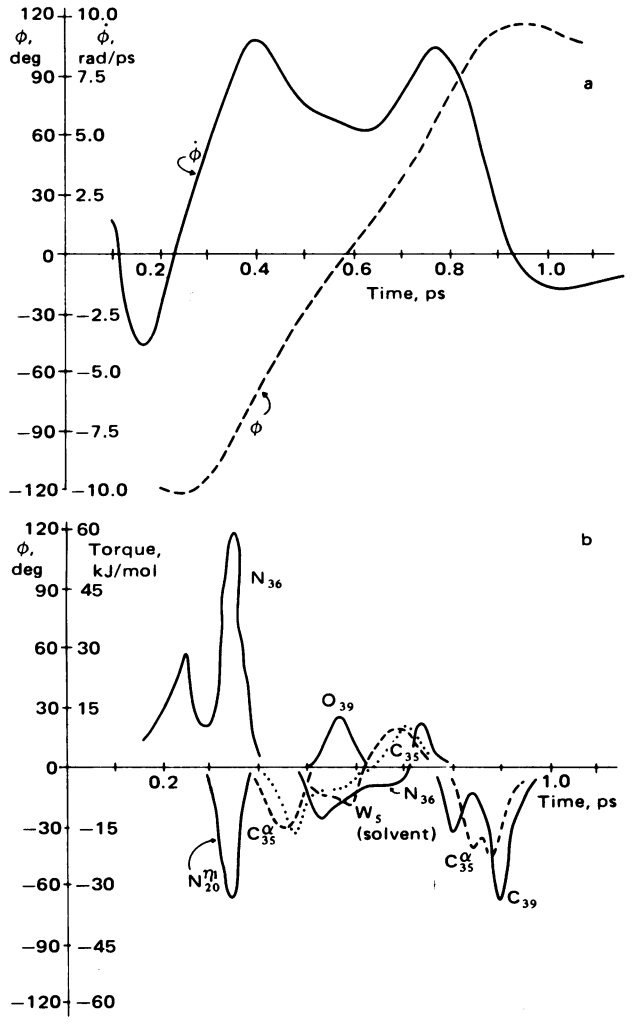


FIG. 2. Barrier crossing trajectory of Tyr-35 in a low-density transition region (type A). (*a*) Ring torsion angle ($\phi$) and torsional angular velocity ($\dot{\phi}$) as a function of time; (*b*) torques exerted on the ring by particular matrix atoms due to nonbonded interactions (contributions from all atoms for which the repulsion exceeded 0.6 kcal/mol are included).

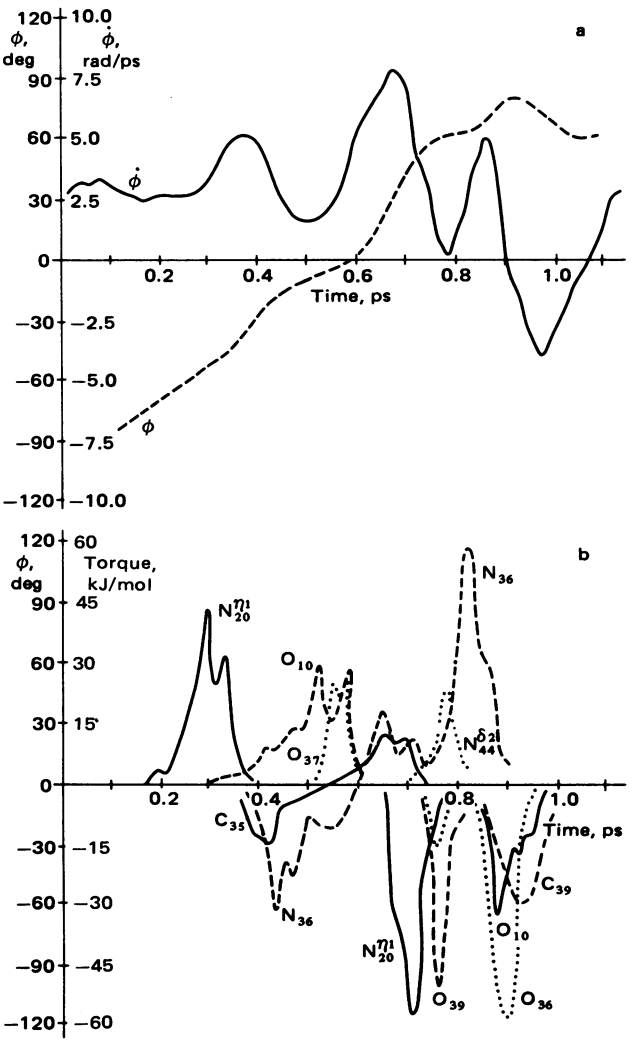


FIG. 3. Barrier crossing trajectory of Tyr-35 in a high-density transition region (type B). (*a*) Ring torsion angle ($\phi$) and torsional angular velocity ($\dot{\phi}$) as a function of time; (*b*) torques exerted on the ring by particular matrix atoms due to nonbonded interactions (contributions from all atoms for which the repulsion exceeded 0.6 kcal/mol are included).

Fluctuations in the bond angles and dihedral angles of Tyr-35 during the ring rotations correspond to those found in the transition state structures (Table 2). Certain bond angle fluctuations are correlated with the occurrence of ring–backbone nonbonded contacts (particularly between $C^{\delta 2}_{35}$ and $N_{36}$). By contrast, the fluctuations in the dihedral angles $\phi_{35}$, $\psi_{35}$ and $\chi^1_{35}$ appear to be uncorrelated with the ring rotations; they are generally similar to what is observed in the equilibrium molecular dynamics simulations of PTI; e.g., $\chi^1_{35}$ fluctuates within 160° ± 30° in all trajectories.

Table 3. Atoms that promote or oppose crossings

| Portion of trajectory | A series | B series |
|---|---|---|
| Ascent ($\phi < -30°$) | P: $O_{10}$, $N^{\eta 1}_{20}$<br>O: $C_{35}$ | P: $C^{\alpha}_{35}$, $N_{36}$<br>O: $C^{\alpha}_{35}$, $C_{35}$ |
| Crossing peak ($-30° < \phi < 30°$) | P: $O_{10}$, $C_{35}$, $N_{36}$<br>O: $N_{36}$ | P: $C_{35}$<br>O: $N_{36}$, W5 |
| Descent ($\phi > 30°$) | P: $N_{36}$<br>O: $O_{10}$, $N^{\eta 1}_{20}$ | P: $N_{36}$<br>O: $C^{\alpha}_{35}$, $C_{39}$ |

P, atoms that promoted crossings in the indicated region in three or more trajectories; O, atoms that opposed crossings in the indicated region in three or more trajectories.

## DISCUSSION

Although the present study provides only preliminary dynamical results for the Tyr-35 ring flips model of an activated process, a number of conclusions are possible. It is clear that the barrier is dominated by interactions between the ring atoms and those of the rest of the protein. A comparison of the two sets of transition configurations obtained by the combined molecular dynamics–constrained Monte Carlo calculation shows that they differ significantly, both in the number of contacts and in the individual atoms involved in opposing or promoting ring rotation. Thus, the sample trajectories described in this paper represent crossings through two local regions of a larger transition state domain; it is indicated schematically in Fig. 4. A calculation of the ring flip rate constant would require extension of the present treatment to include a more complete sampling of the transition region and of trajectories for different configurations in that region. In addition, as already outlined in the introduction, an evaluation of the equilibrium probability of

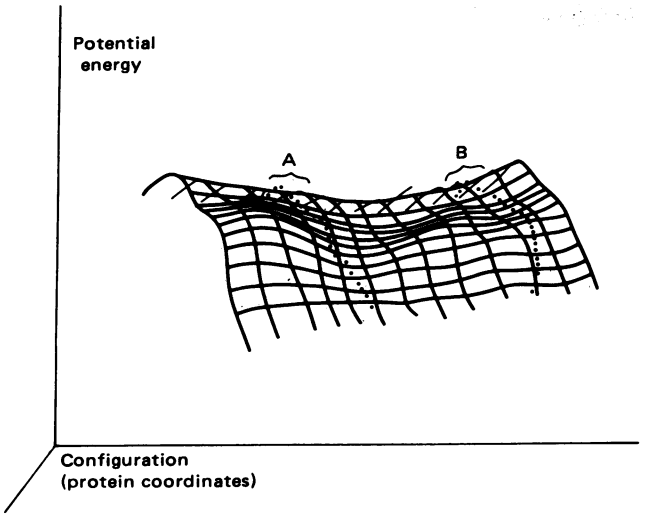


FIG. 4. Protein energy ridge separating the two valleys that correspond to stable orientations of the Tyr-35 ring. Trajectories that cross through two regions (A and B) of this ridge have been sampled; two such trajectories are indicated by dotted lines. Trajectories crossing through region A may exhibit some slowing down due to the nearby bulge, which is the result of nonbonded repulsion between ring and protein matrix atoms.

each configuration is needed. The latter can be achieved by sampling successive portions of space that connect the transition region with that in the neighborhood of the equilibrium geometry (19).

An important result common to all of the trajectories is that the stresses arising from nonbonded repulsion (e.g., that between $C_{35}^{\delta 2}$ and $N_{36}$) are relaxed during the dynamics by local configurational adjustments (such as those reflected in the bond angle deformations) on a time scale short compared to the ring reorientation. This provides support for the use of adiabatic calculations to estimate the potential energy of conformational barriers and helps to explain why such estimates are in good agreement with experiment (13, 14). Examination of the trajectories shows further that the torques exerted on the ring act for very short times, so that an impulsive model may be appropriate as a starting point in an analytical description of the ring dynamics (16, 27). The essential effect of the interaction is to suddenly change the angular velocity of the ring atoms without any displacement during the interaction time.

In the barrier-crossing trajectories, damping or frictional effects are evident, although they are not strong enough to result in Brownian behavior. The repulsive nonbonded interactions between the ring and protein matrix atoms played a crucial role in producing and subsequently halting rotation of the ring and in determining the detailed character of the barrier-crossing dynamics. In several trajectories, particularly those of the A series (in which the local density of the matrix is relatively high), the torsional motion of the ring was nearly halted one or more times by these nonbonded interactions. These results are in accord with predictions based on the properties of equilibrium torsional fluctuations of tyrosine rings in PTI (16). For other types of activated conformational changes, the relative importance of frictional damping may be expected to increase with the effective size of the displaced group and with the width of the barrier.

It is hoped that this preliminary study has provided some insight into the nature of the dynamics of activated processes in proteins. More extensive calculations on the ring rotation problem, as well as applications to enzymatic reactions that involve bond breaking and formation, will be presented in future publications.

We thank C. H. Bennett for helpful discussions. The research was supported by grants from the National Science Foundation and National Institutes of Health. J.A.M. was supported by National Institutes of Health Postdoctoral Fellowship 1 F32 GM05717-01A1.

1. Jencks, W. P. (1969) *Catalysis in Chemistry and Enzymology* (McGraw-Hill, New York).
2. Campbell, I. D., Dobson, C. M. Moore, G. R., Perkins, S. J. & Williams, R. J. P. (1976) *FEBS Lett.* **70**, 96–100.
3. Snyder, G. H., Rowan, R., III., Karplus, S. & Sykes, B. D. (1975) *Biochemistry* **14**, 3765–3777.
4. Wagner, G., DeMarco, A. & Wüthrich, K. (1976) *Biophys. Struct. Mech.* **2**, 139–158.
5. Austin, R. H., Beeson, K. W., Eisenstein, L., Frauenfelder, H. & Gunsalus, I. C. (1975) *Biochemistry* **14**, 5355–5373.
6. Eisenstein, L. (1977) *Int. J. Quantum Chem. Symp.* **4**, 363–374.
7. Knowles, J. R. & Albery, W. J. (1977) *Acc. Chem. Res.* **10**, 105–111.
8. McCammon, J. A., Gelin, B. R. & Karplus, M. (1977) *Nature (London)* **267**, 585–590.
9. Richards, F. M. (1977) *Annu. Rev. Biophys. Bioeng.* **6**, 151–176.
10. Kramers, H. A. (1940) *Physica* **7**, 284–304.
11. Skinner, J. L. & Wolynes, P. G. (1978) *J. Chem. Phys.* **69**, 2143–2150.
12. Northrup, S. H. & Hynes, J. T. (1978) *J. Chem. Phys.* **69**, 5246–5260.
13. Gelin, B. R. & Karplus, M. (1975) *Proc. Natl. Acad. Sci. USA* **72**, 2002–2006.
14. Hetzel, R., Wüthrich, K., Deisenhofer, J. & Huber, R. (1976) *Biophys. Struct. Mech.* **2**, 159–180.
15. Karplus, M. & McCammon, J. A. (1979) *Nature (London)* **277**, 578.
16. McCammon, J. A., Wolynes, P. G. & Karplus, M. (1979) *Biochemistry* **18**, 927–942.
17. Keck, J. C. (1962) *Discuss. Faraday Soc.* **33**, 173–182.
18. Anderson, J. B. (1973) *J. Chem. Phys.* **58**, 4684–4692.
19. Bennett, C. H. (1975) in *Diffusion in Solids*, eds. Burton, J. J. & Nowick, A. S. (Academic, San Francisco), pp. 73–113.
20. Gelin, B. R. & Karplus, M. (1979) *Biochemistry* **18**, 1256–1268.
21. Kushick, J. & Berne, B. J. (1977) in *Statistical Mechanics, Part B*, ed. Berne, B. J. (Plenum, New York), pp. 41–63.
22. Valleau, J. P. & Whittington, S. G. (1977) in *Statistical Mechanics, Part A*, ed. Berne, B. J. (Plenum, New York), pp. 137–168.
23. Kennard, E. H. (1938) *Kinetic Theory of Gases* (McGraw-Hill, New York).
24. Johnston, H. S. (1966) *Gas Phase Reaction Rate Theory* (Ronald, New York), pp. 48–54.
25. Gear, C. W. (1971) *Numerical Initial Value Problems in Ordinary Differential Equations* (Prentice-Hall, Englewood Cliffs, NJ).
26. Deisenhofer, J. & Steigemann, W. (1975) *Acta Crystallogr. Sect. B* **31**, 238–250.
27. Chandler, D. (1974) *Acc. Chem. Res.* **7**, 246–251.